Subcellular Distribution of Rhodamine-Actin Microinjected into Living Fibroblastic Cells

STEPHEN D. GLACY
Division of Biology, Kansas State University, Manhattan, Kansas 66506. Mr. Glacy's present address is The University of Kansas, College of Health Sciences and Hospital, Kansas City, Kansas 66103.

ABSTRACT   The time course and pattern of incorporation of rhodamine-labeled actin microinjected into cultured fibroblastic cells were examined by fluorescence microscopy. Following microinjection, the fluorescent probe was incorporated rapidly into ruffling membranes, and within 5 min faintly fluorescent stress fibers were observed. Levels of fluorescence in ruffling membranes then tended to remain constant while fluorescence of the stress fibers continued to increase until ~20-min postinjection. Small, discrete regions of some microinjected cells displayed high levels of fluorescence that appeared initially ~5–10 min postinjection. I observed these small areas of intense fluorescence frequently near the cell periphery, which corresponded to focal contacts when examined with interference reflection optics. The results of this study show that a relationship exists between patterns of fluorescent actin incorporation in these cells and cellular areas or structures presumed to play a role in cell movement. These findings suggest that actin within stress fibers and the microfilament network of ruffling membranes undergoes a rapid turnover that may relate directly to the motility of the cell.

Actin may comprise as much as 15% of total cellular protein in nonmuscle cells (1), and has been implicated in such dynamic cellular activities as cytokinesis (2), membrane ruffling (3, 4), and cell spreading in vitro (5). Evidence for actin involvement in these functions stems mainly from observations that in areas of high motile activity, such as the cleavage furrow in dividing cells or the leading edge in actively moving cells, actin is present in a form and distribution that may readily lend itself to force generation (see reference 3 for a review).

A combination of techniques, including biochemical studies (6), electron microscopy (3, 4, 7), and fluorescence microscopy (5, 7), has demonstrated that actin exists in cultured nonmuscle cells in both the polymerized and nonpolymerized forms. Nonpolymerized actin, which may account for 35–50% of the total actin in nonmuscle cells (6), is probably not present as soluble G-actin, but more likely is complexed with one or more of the numerous actin-binding proteins of nonmuscle cells (8). Since the general ionic conditions of the cytoplasm are such that 98% of cellular actin should be in the filamentous form (9), it is obvious that nonmuscle cells possess regulatory systems that maintain large portions of their actin in a nonpolymerized state, possibly for employment in dynamic cellular processes by controlled rapid polymerization.

Recently, Wang and Taylor introduced the technique of fluorescent analog cytochemistry involving microinjection of fluorochrome-labeled cellular components into cells and subsequent determination of their fate (10, 11). Other investigators have extended this approach to the study of cellular contractile functions by introducing a variety of proteins and substances into cells: actin (12–19), tropomyosin (20), calmodulin (21), tubulin (22), 130,000-mol-wt protein (23), α-actinin (24–26), antiactin antibodies (27), anti-intermediate filament antibodies (28, 29), antimyosin antibodies (30, 31), aequorin (32), phalloidin (33–37), calcium (38), chlorotetracycline (39), and N-ethylmaleimide-modified heavy meromyosin (40).

In the present study, I examined some of the dynamic properties of rhodamine-labeled actin microinjected into cultured chick fibroblastic cells. My results indicate that exogenous rhodamine-actin is rapidly incorporated into specific subcellular structures and areas containing F-actin and possibly playing a role in cell motility. These findings suggest that the molecular exchange of actin subunits in living cells is a dynamic and continuous process.

MATERIALS AND METHODS

Cell Culture Procedures: Heart ventricles from 12–14-d chick embryos were minced in sterile calcium- and magnesium-free Saline G (CMF Sal

G), and enzymatically dissociated into single cells with 0.2% trypsin in CMF Sal G for 30 min at 37°C. Digestions were terminated by addition of an equal volume of F-12 nutrient medium containing 10% fetal calf serum, 30 μg/ml penicillin G, and 50 μg/ml streptomycin sulfate. Cell suspensions were filtered through single layers of Nitex cloth, collected by centrifugation, resuspended in fresh nutrient medium, and plated into 60-mm diameter Falcon tissue culture dishes (Falcon Labware, Oxnard, CA). The dishes were kept in a humid atmosphere of 5% CO_2/95% air at 37°C. Before microinjection, primary cultures were trypsinized and replated at lower densities onto glass coverslips and cultured for an additional 24-48 h.

Fluorescent Labeling of Actin: Skeletal muscle actin was prepared from an acetone powder of chicken breast muscle (41) and dialyzed against buffer G (2 mM Tris-HCl, 0.4 mM ascorbate, 0.2 mM ATP, 0.1 mM $CaCl_2$, pH 8.0) to obtain G-actin. Concentrations of unlabeled G-actin were determined spectrophotometrically by absorption at 290 nm using an extinction coefficient of 0.63 ml mg^{-1} cm^{-1} (42). Concentrations of rhodamine-actin were measured by the Bradford protein assay (43), which was standardized against a spectrophotometrically determined G-actin solution. 10 mg of iodoacetami-dotetramethyl rhodamine (Research Organics, Cleveland, OH) was placed into 0.5 ml of acetone, vortexed, and added to 3 ml of buffer G containing 8 mM ATP at pH 10.5-11. This dye solution was added dropwise to 12-15 mg of G-actin in 4 ml of buffer G. Mixtures were titrated to pH 8.5 with 0.1 N NaOH and stirred for 2 h at room temperature. The actin was polymerized by addition of 3 M KCl and 1 M $MgCl_2$ to final concentrations of 100 and 2 mM, respectively, and sedimented by centrifugation at 100,000 g for 3 h. F-actin pellets were depolymerized in 600 mM KI, desalted on a Sephadex G-25 column (42), and clarified by centrifugation at 100,000 g for 2 h. Rhodamine-actin preparations were taken through another polymerization/deploymeriza-tion cycle and stored at 4°C for no more than 24 h before use in experiments. Dye/protein ratios were determined to be 0.4-0.6 using an extinction coefficient of 2.4 × 10^{-4} cm^{-1} M^{-1} at 555 nm for rhodamine-actin (44). Viscosities of labeled and unlabeled F-actin solutions were measured using a Cannon-Man-ning semi-microviscometer Model 150 (Cannon Instrument Co., State College, PA) (42).

Microinjection and Microscopy: The microinjection system used was similar to that described by Diacumakos (45). Coverslips with attached cells were inverted to form the top of a microinjection chamber, which consisted of a U-shaped plastic support resting upon a 45 × 50 mm No. 2 coverglass. During microinjection and observations within 5 min postinjection, chambers were filled with Saline G. For observations during later periods of the experiments, Saline G was replaced with nutrient medium. Injection micropipettes were formed from 0.9 (inner diameter) × 1.2 (outer diameter) × 100 mm Omega Dot capillary tubes (Frederick Haer & Co., Brunswick, ME) which had been soaked consecutively in acetone and nitric acid, and rinsed extensively with three times glass-distilled water and dried. Micropipettes were pulled on a DKI 700C capillary puller (David Kopf Instruments, Tujunga, CA) and shaped on a laboratory-made microforge. Rhodamine-actin (2-3 mg/ml in buffer G) was backloaded into micropipettes which then were mounted onto a micro-manipulator (E. Leitz, Inc., Rockleigh, NJ). Injections, observations, and photography were performed on a Zeiss Standard microscope equipped with epifluorescence optics. Interference reflection microscopy was done as previously described (46). Exposures were taken on Ilford XP-1 35 mm film and developed for 6.5 min at 40°C in Ilford XP-1 chemicals.

The amount of rhodamine-actin microinjected into cells was estimated by the following means. Cells were injected in their perinuclear region with the micropipette remaining in the cell until ~20-30% of the cell area, as micro-scopically viewed, displayed the injection fluid. By approximating cell area to cell volume, and knowing the concentrations of rhodamine-actin (2-3 mg/ml) and endogenous actin in fibroblasts (8 mg/ml) (47), the injected rhodamine-actin was estimated to represent roughly 11% of total endogenous actin (30% × 3 mg/ml/100% × 8 mg/ml = 0.11).

RESULTS

Controls

VISCOSITY OF ACTIN SOLUTIONS: The ability of actin to polymerize with a concomitant increase in viscosity is a fundamental biochemical property of the protein. Ostwald capillary viscometry was used to compare the viscometric properties of unlabeled actin and rhodamine-actin. Fig. 1 summarizes these studies and indicates that in the protein concentration range tested, both unlabeled and labeled prep-arations displayed similar viscosities.

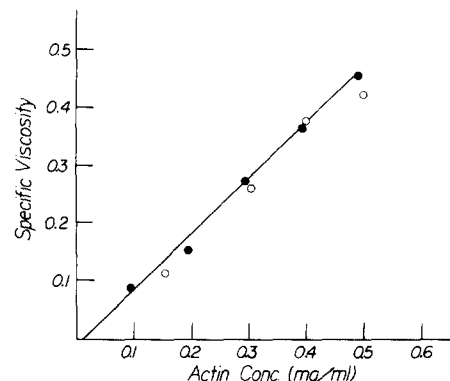NONSPECIFIC BINDING OF RHODAMINE-ACTIN: In

FIGURE 1 Ostwald capillary viscometry of labeled (O) and unla-beled (●) F-actin solutions. G-actin solutions were polymerized by the addition of 3 M KCl and 1 M $MgCl_2$ to final concentrations of 100 and 2 mM, respectively, then incubated for 6 h at 25°C. The solid line indicates the slope generated by the unlabeled F-actin preparations. Each point represents the average of two independent samples, each of which was measured twice.

a recent report, rhodamine labeled α-actinin was shown to bind to stress fibers in demembranated fibroblasts in an arrangement similar to that of immunofluorescence with anti-α-actinin antibodies and to microinjected α-actinin (48). To provide evidence that the patterns I obtained in microinjected cells reflected active cell-mediated actin incorporation and not passive binding of rhodamine-actin to cytoplasmic struc-tures, cardiac myocytes, and fibroblasts were permeabilized with 0.5% Triton X-100 and 0.37% formaldehyde in PBS for 5 min, and postfixed in 3.7% formaldehyde in PBS for 20 min, before incubation with rhodamine-actin (200 μg/ml) and buffer G for 10 min. Fig. 2 shows that this treatment resulted in low uniform fluorescence in the cytoplasm, com-paratively higher nuclear fluorescence and no discernible binding of the probe to either stress fibers or myofibrils. However, fixation of these cells introduces the possibility that any sites providing for passive binding of the fluorescent probe were destroyed.

MICROINJECTION OF FITC-OVALBUMIN: As a sec-ond control to demonstrate that patterns of fluorescence in microinjected cells represented functional incorporation of rhodamine-actin, I injected living fibroblastic cells with FITC-ovalbumin, a noncytoskeletal protein. Upon injection this protein diffused freely into the cytoplasm and within minutes achieved a fluorescence distribution that did not change over the observation period of 1 h (Fig. 3). Phase-contrast micros-copy of these injected cells showed numerous stress fibers (Fig. 3a, arrows) that were not fluorescent when the same cells were examined under UV illumination. Some regions of cells microinjected with FITC-ovalbumin appeared less fluo-rescent, especially along the periphery. The fluorescent cell in Fig. 3b showed a marked transition in fluorescence intensity that may exist due to a change in cell thickness or the presence of cellular structures in the perimeter region which excluded FITC-ovalbumin (Fig. 3b, arrow).

SDS PAGE OF RHODAMINE-ACTIN: To critically inter-pret fluorescence patterns observed in microinjected cells it was important to ascertain the level of fluorescent substances that were not associated with polymerization competent rho-damine-actin. At least four sources of nonspecific fluorescence were possible: (a) free dye: any rhodamine that had not reacted covalently with actin, yet was carried through the purification procedures; (b) degradation products of rhodamine-actin:
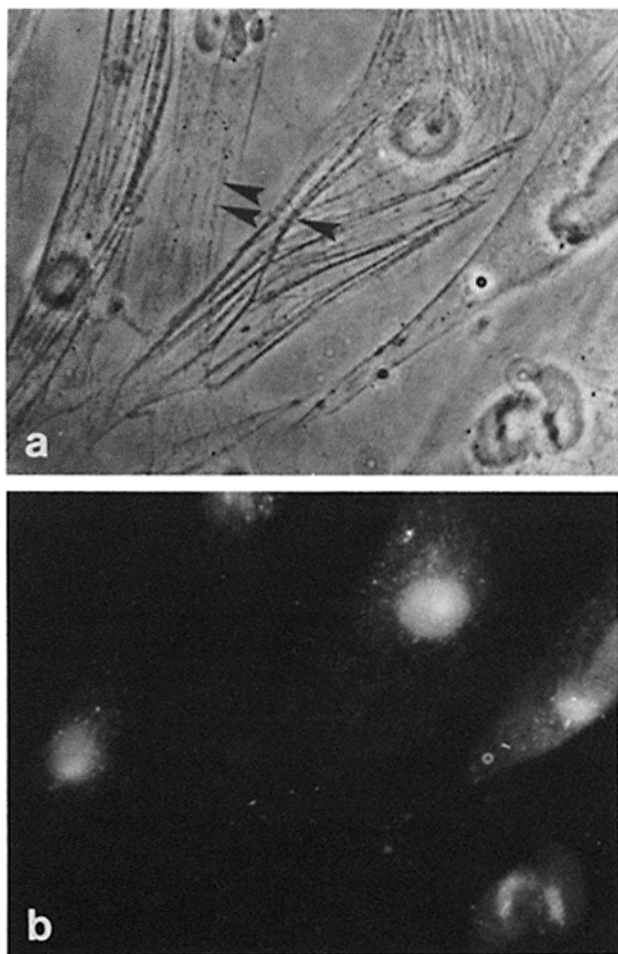
FIGURE 2 Phase-contrast and matching fluorescence images of permeabilized, fixed cells incubated with rhodamine-actin. The phase-contrast micrograph (a) demonstrates the numerous myofibrils of the myocytes (single arrowhead) and stress fibers of the fibroblastic cells (double arrowheads). The matching fluorescence photomicrograph (b) shows that neither the myofibrils nor the stress fibers bind the rhodamine-actin. × 640.
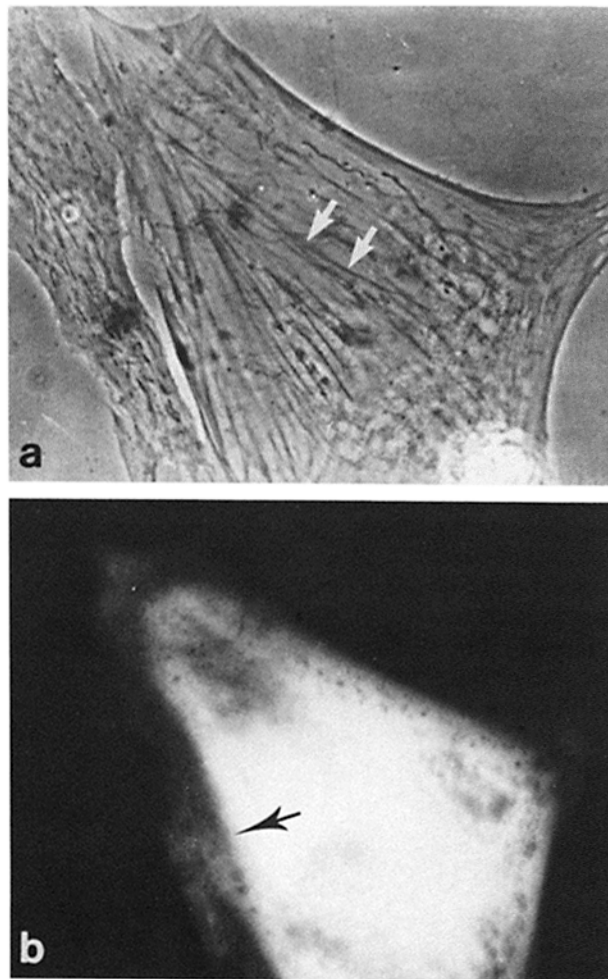

FIGURE 3 Phase-contrast and matching fluorescence photomicrographs of a fibroblastic cell 1 h after microinjection of FITC-ovalbumin. By phase-contrast microscopy numerous stress fibers were observed (a, arrows) which were not fluorescent when the same cell was examined by epifluorescence illumination. Regions along the perimeter of this cell were much less fluorescent than central portions and a distinct transition existed between the fluorescence intensities of these areas (b, arrow). × 750.

spontaneous or proteolytic degradation of rhodamine-actin, resulting in nonfunctional fluorescent peptides; (c) trace protein contaminants: such as tropomyosin, which may have contaminated actin preparations and were labeled with the fluorescent dye; and (d) denatured rhodamine-actin: actin that had denatured during the labeling and purification procedure (different batches of dye were found to contribute significantly to this source of contamination). The purity of rhodamine-actin was monitored by gel electrophoresis. Fig. 4 shows rhodamine-actin subjected to electrophoresis in a 10% SDS polyacrylamide gel. Other than very slight fluorescence associated with the dye front, only the actin band showed fluorescence. Electrophoresis in SDS polyacrylamide gels cannot reveal whether actin migrating at 42,000 mol wt is native or denatured. To ensure the biochemical integrity of the probe, I subjected the rhodamine-actin to at least two polymerization/depolymerization cycles after labeling with iodoacetamidotetramethyl rhodamine, and always used it within 24 h for microinjection.

Time Course of Rhodamine-Actin Incorporation

Results reported in this paper are based on observations of at least 300 microinjected fibroblastic cells. Immediately fol-
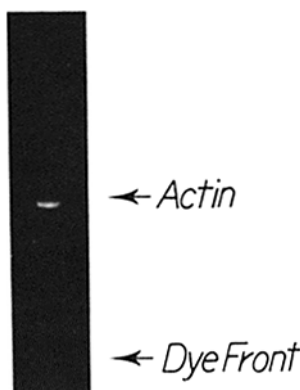

FIGURE 4 Fluorescence photograph of rhodamine-actin electrophoresed in SDS polyacrylamide. Other than small amounts of fluorescence at the dye front and the fluorescence associated with actin, the lane shows no other fluorescent bands.

lowing microinjection, rhodamine-actin spread rapidly through the cytoplasm of fibroblastic cells and resulted in uniform cellular fluorescence. Less than 5 min after injection there was a pronounced fluorescence increase in cell areas corresponding to ruffling membranes, with maximum fluorescence levels obtained in these regions ~5-min postinjec-

tion (Fig. 5 b). In some cells, the difference in fluorescence intensity between the ruffling membrane and more interior areas of the cell was quite substantial (Fig. 5 b). Some of the interior cellular regions, particularly those directly adjacent to the ruffling membrane, were as nonfluorescent as the surrounding substrate. Peripheral fluorescence in areas of the ruffling membrane was of uniform width (single arrow, Fig. 5 b) or quite varying in width (double arrows, Fig. 5 b).

Fluorescence in stress fibers initially appeared ~5-min postinjection (Fig. 5 b), and by 10 min was quite prominent (Fig. 5 d). The fluorescence level of stress fibers continued to increase until ~20-min postinjection, then tended to remain constant. Additionally, incorporation of rhodamine-actin into stress fibers was simultaneous along the entire length of the fibers (with the exception of some stress fiber termini, as noted in the next section). Fluorescence incorporation did not originate at one end of a stress fiber and progress its length. No periodicities of fluorescence distribution in stress fibers were observed. In some cells, polygonal fiber networks (47) also incorporated rhodamine-actin with rates similar to stress fibers (data not shown).

During the course of these experiments it was noted that
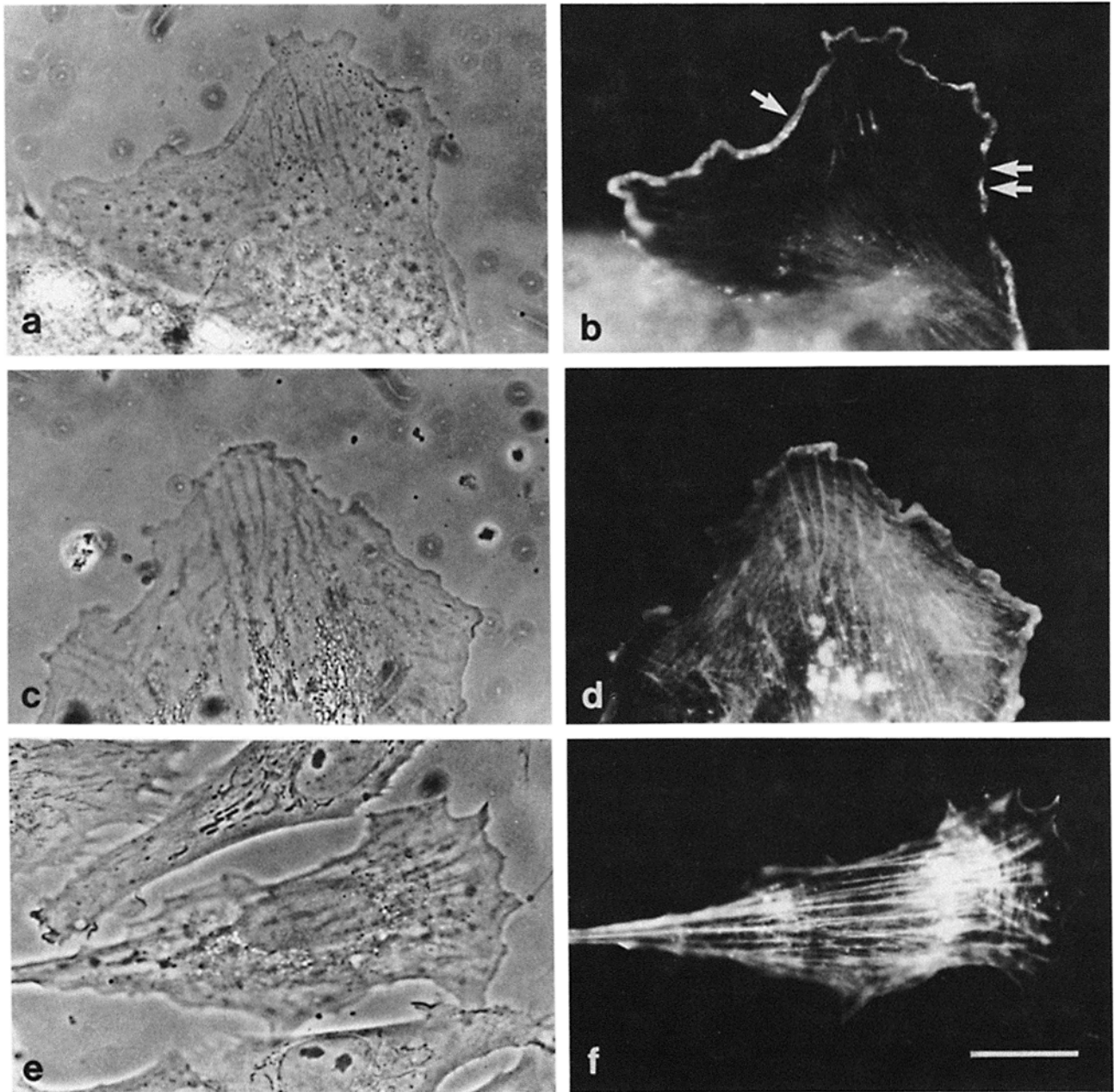

FIGURE 5   Phase-contrast and corresponding fluorescence images of chick heart fibroblastic cells microinjected with rhodamine-actin. Time points following injection are 5 min (a and b), 10 min (c and d), and 1 h (e and f). At 5-min postinjection, a distinct band of fluorescence is evident along the cell periphery in the region of the ruffling membrane (b), which may be of uniform width (single arrow) or of various widths (double arrows). By 10 min after microinjection, fluorescence can be seen in both the ruffling membrane and stress fibers. e and f show a wedge-shaped cell at 1-h postinjection, demonstrating incorporation of most rhodamine-actin into stress fibers. Bar, 20 μm. X 820.

the degree of fluorescent actin incorporation into stress fibers varied widely among microinjected cells. In some cells the injected probe remained diffuse with little stress fiber incorporation. Other cells incorporated most of the injected probe into stress fibers leaving very little interfibrillary cytoplasmic fluorescence. In general, a correlation existed between cellular morphology and distribution of rhodamine-actin. Polygonal-shaped cells usually incorporated most of the injected rhodamine-actin into stress fibers while wedge-shaped cells frequently displayed a more uniform fluorescence pattern. However, these generalities did not hold for all cells observed. Fig. 5, e and f, show a wedge-shaped cell at 1 h postinjection. Most of the rhodamine-actin had been incorporated into the many stress fibers oriented with the long axis of the cell. Note especially the very low levels of fluorescence in the interfibrillary space of the perinuclear region, and the lack of fluorescence in the putative leading edge. This example demonstrates that cell shape alone is not a reliable indicator of rhodamine-actin distribution and other factors such as rate of cell movement are likely to influence these patterns.

Rhodamine-Actin Incorporation and Focal Contacts

Of the cells microinjected with rhodamine-actin, many showed particularly bright patches of fluorescence that were noticed shortly after injection. These patches showed a striking similarity to fluorescence patterns seen in cells stained with antibodies to vinculin, a protein selectively present in focal contacts (46). This prompted an examination of the cells by interference reflection microscopy to study the relationship between these patches and the substrate contact points of the cells. Interference reflection optics revealed that many of the fluorescent patches corresponded to focal contacts and appeared to be at stress fiber termini (Fig. 6, arrows). Additionally, these areas frequently corresponded to phase-dense patches (Fig. 6a, arrow).

These patches were most conspicuous in the time period of 5–10 min postinjection, which was slightly before stress fibers reached their maximum levels of fluorescence. In cells examined 20–30 min after injection, the fluorescent patches decreased in relative prominence as stress fibers that led to such focal contacts progressively incorporated increasing amounts of rhodamine-actin.

DISCUSSION

This paper presents information demonstrating that fibroblastic cells rapidly incorporate rhodamine-actin into selective subcellular structures that have been implicated in cell motility and cytoskeletal functions. Leading edges and ruffling membranes are areas commonly present in tissue culture cells undergoing locomotion, and in this study, showed a marked increase in fluorescence following microinjection, reaching a maximum level by 5-min postinjection. Stress fibers usually are assigned a cytoskeletal role because of the inverse relationship between their number in a cell and the rate of cellular movement (5). In the present study, stress fibers began to show fluorescence ~5-min postinjection and, in contrast to ruffling membranes, continued to increase in fluorescent intensity until a maximum level was achieved ~20-min postinjection.

Results described in this manuscript corroborate and extend findings recently reported by Kreis et al. (18). In their study of rhodamine-actin dynamics in chicken gizzard cells by fluorescence photobleaching recovery, they discovered that the leading edge displayed the highest rate of rhodamine-actin mobility of all cellular domains studied. Additionally, their reported half-time of 10 min for fluorescence recovery in stress fibers agrees well with my observation that maximum levels of fluorescence in stress fibers were achieved by 20-min postinjection.

Several possibilities exist that may explain the relatively faster incorporation of actin into ruffling membranes. Microfilaments of the ruffling membrane are usually present as a network of individual filaments, rather than as the bundles characterizing stress fibers (4). Thus, the filaments of this region are probably more accessible to microinjected actin. The faster rate of fluorescence increase, therefore, may simply reflect higher availability of polymerization sites in filaments of the ruffling membrane than in those of stress fibers. Alternatively, faster incorporation rates in the ruffling membrane may stem from the high motile activity characterizing the area. Breakdown, assembly, and rearrangement of actin filaments probably are required for these motile activities, which include extension and retraction of the lamellapodium. Increased rates of incorporation, therefore, may reflect increased filament turnover, which is presumed to require a readily available pool of G-actin.
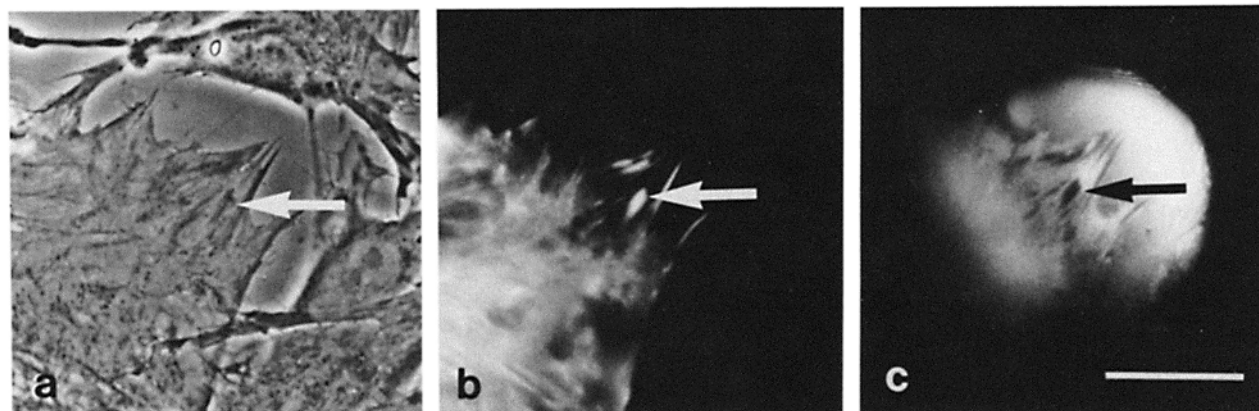

FIGURE 6 Phase-contrast, fluorescence, and interference reflection images of a portion of a chick heart fibroblastic cell microinjected with rhodamine-actin at 10-min postinjection. By fluorescence microscopy (b) bright patches of fluorescence can be seen at and near the cell perimeter which correspond to phase-dense regions seen by phase-contrast microscopy (a) and to focal contacts seen by interference reflection microscopy (c). Bar, 20 μm. × 900.

Morphologically, stress fibers are relatively unchanging structures. It is possible to observe single stress fibers in some cells by phase-contrast optics for several hours without noting drastic changes in length or appearance (3). Thus, the swift appearance of fluorescence in stress fibers of microinjected cells is surprising and suggests that these morphologically stable structures are in fact relatively dynamic at a molecular level. Moreover, the incorporation of fluorescence uniformly along the length of stress fibers suggests that they contain numerous polymerization sites, and hence may be comprised of many short microfilaments. Presently, the exact form of actin as it is incorporated into stress fibers is unknown. It may be recruited as simple G-monomers, or the cell may construct oligomers or short fragments outside of stress fibers with subsequent incorporation. Focal contacts are discrete areas where the underside of the cell is within 15 nm of the substrate. These areas usually correspond to adhesion plaques and are generally located at the terminating tips of microfilament bundles (50). The results presented here demonstrate that there is an early and distinct recruitment of rhodamine-actin into focal contacts following microinjection of fibroblastic cells. It is not clear whether this selective incorporation represents a molecular exchange that is of functional significance, or merely reflects a high number of potential polymerization sites in the area.

Metabolic half-lives of actin and myosin in cultured fibroblasts have been reported to be a minimum of 2.5 d (51). Therefore, the rapid appearance of rhodamine-actin in F-actin-containing structures of microinjected cells probably does not represent metabolic protein turnover (i.e., biosynthesis and degradation). More likely, results of the present study suggest a constant cycling of actin through these structures, with little protein degradation. Additionally, the width of ruffling membrane fluorescence, as well as stress fiber length, displayed no discernible increase during incorporation of rhodamine-actin. It seems likely then that as rhodamine-actin molecules were being incorporated, other actin molecules were removed. Filamentous actin in vitro undergoes a continuous exchange with available G-actin, without a net change of overall filament length (47). My findings suggest a similar phenomenon for actin filaments in vivo. Immediately following microinjection, rhodamine-actin would become part of the cell's nonfilamentous pool of actin and serve as a tracer for that pool. The exchange process at this point would be represented by incorporation of both rhodamine-actin and endogenous unlabeled actin from the cell's existing nonpolymerized actin pool, and removal of endogenous unlabeled actin molecules from filaments. Subsequent to this would be a period of equilibration during which rhodamine-actin would be uniformly distributed into both the polymerized and nonpolymerized actin pools of the cell. The exchange process following equilibration of the probe would be represented by equal numbers of rhodamine-actin molecules entering and leaving the filaments. A mechanism of this sort would explain the rapid appearance of fluorescence in stress fibers and ruffling membranes immediately following injection and its subsequent persistence. I have noted similar rhodamine-actin incorporation dynamics in myofibrils of microinjected cardiac myocytes (19), indicating that the basic subunit exchange mechanism of F-actin may be the same regardless of cell type.

The results of the present study support the increasingly widespread notion of the dynamic nature of actin in vertebrate cells. A considerable portion of the actin in nonmuscle cells

exists in the nonpolymerized state (6), despite general cytosolic ionic conditions which prescribe that most of the actin should be in a filamentous form. The numerous actin binding proteins may serve to maintain this large pool of nonpolymerized actin (8). Therefore, it seems likely that a balance of factors affects the state of actin polymerization in the cytosol: ionic conditions favoring polymerization versus actin binding proteins maintaining filament length and favoring nonpolymerized forms. With this background one must then consider the possible perturbing effects of microinjected rhodamine-actin. The introduction of pure G-actin into the cytoplasm is bound to upset, to an unknown degree, the equilibrium between polymerized and nonpolymerized actin. Due to intracellular ionic conditions the tendency will be for the injected actin to polymerize immediately. However, at the injection concentrations used in this study (2-3 mg/ml), the initial fluorescence was always uniform, which may represent a nonpolymerized state. If this is, in fact, a nonpolymerized form of actin, then it suggests a sufficient abundance of actin-binding proteins in the cell to prevent immediate polymerization. It is interesting to note, however, that cells do appear to have definite limits to their ability to control injected actin. Microinjection of rhodamine-actin at concentrations three times higher than those used in the present study resulted in immediate formation of long wavy filaments or structures resembling actin paracrystals (data not shown). These unusual actin structures were observed in cells up to 2 h postinjection, but no long-term study has been done to see if cells eventually depolymerized them.

REFERENCES

1. Bray, D., and C. Thomas. 1975. The actin content of fibroblasts. *Biochem. J.* 147:221–228.
2. Schroeder, T. E. 1973. Actin in dividing cells: contractile ring filaments bind heavy meromyosin. *Proc. Natl. Acad. Sci. USA.* 70:1688–1692.
3. Buckley, I. K. 1981. Fine-structural and related aspects of nonmuscle-cell motility. *Cell Muscle Motil.* 1:135–203.
4. Small, J. V., G. Isenberg, and J. E. Celis. 1978. Polarity of actin at the leading edge of cultured cells. *Nature (Lond.).* 272:638–639.
5. Herman, I. M., N. J. Crisona, and T. D. Pollard. 1981. Relation between cell activity and the distribution of cytoplasmic actin and myosin. *J. Cell Biol.* 90:84–91.
6. Blikstad, I., and L. Carlsson. 1982. On the dynamics of the microfilament system in HeLa cells. *J. Cell Biol.* 93:122–128.
7. Willingham, M. C., S. S. Yamada, P. J. A. Davies, A. V. Rutherford, M. G. Gallo, and I. Pastan. 1981. Intracellular localization of actin in cultured fibroblasts by electron microscopic immunocytochemistry. *J. Histochem. Cytochem.* 29:17–37.
8. Weeds, A. 1982. Actin-binding proteins: regulators of cell architecture and motility. *Nature (Lond.)* 296:811–816.
9. Korn, E. D. 1978. Biochemistry of actomyosin-dependent cell motility. *Proc. Natl. Acad Sci. USA.* 75:588–599.
10. Wang, Y.-L., J. M Heiple, and D. L. Taylor. 1982. Fluorescent analog cytochemistry of contractile proteins. *Methods Cell Biol.* 25:1–11.
11. Taylor, D. L., and Y.-L. Wang. 1980. Fluorescently labelled molecules as probes of the structure and function of living cells. *Nature (Lond.).* 284:405–410.
12. Sanger, J. W., J. M. Sanger, T. E. Kreis, and B. M. Jockusch. 1980. Reversible translocation of cytoplasmic actin into the nucleus caused by dimethyl sulfoxide. *Proc. Natl. Acad. Sci. USA.* 77:5268–5272.
13. Birchmeier, C., T. E. Kreis, H. M. Eppenberger, K. H. Winterhalter, and W. Birchmeier. 1980. Corrugated attachment membrane in WI-38 fibroblasts: alternating fibronectin

fibers and actin-containing focal contacts. *Proc. Natl. Acad. Sci. USA.* 77:4108–4112.

14. Kreis, T. E., K. H. Winterhalter, and W. Birchmeier. 1979. *In vivo* distribution and turnover of fluorescently labeled actin microinjected into human fibroblasts. *Proc. Natl. Acad. Sci. USA.* 76:3814–3818.

15. Taylor, D. L., Y.-L. Wang, and J. M. Heiple. 1980. Contractile basis of ameboid movement. VII. The distribution of fluorescently labeled actin in living amebas. *J. Cell Biol.* 86:590–598.

16. Gawlitta, W., W. Stockem, J. Wehland, and K. Weber, 1980. Organization and spatial arrangement of fluorescein-labeled native actin microinjected into normal locomoting and experimentally influenced *Amoeba proteus. Cell Tissue Res.* 206:181–191.

17. Wang, Y.-L., and D. L. Taylor. 1979. Distribution of fluorescently labeled actin in living sea urchin eggs during early development. *J. Cell Biol.* 82:672–679.

18. Kreis, T. E., B. Geiger, and J. Schlessinger. 1982. Mobility of microinjected rhodamine actin within living chicken gizzard cells determined by fluorescence photobleaching recovery. *Cell.* 29:835–845.

19. Glacy, S. D. 1983. Pattern and time course of rhodamine-actin incorporation in cardiac myocytes. *J. Cell Biol.* 96:1164–1167.

20. Wehland, J., and K. Weber. 1980. Distribution of fluorescently labeled actin and tropomyosin after microinjection in living tissue culture cells as observed with TV image intensification. *Exp. Cell Res.* 127:397–408.

21. Hamaguchi, Y., and F. Iwasa. 1980. Localization of fluorescently labeled calmodulin in living sea urchin eggs during early development. *Biomed. Res.* 1:502–509.

22. Keith, C. H., J. R. Feramisco, and M. Shelanski. 1981. Direct visualization of fluorescein-labeled microtubules in vitro and in microinjected fibroblasts. *J. Cell Biol.* 88:234–240.

23. Burridge, K., and J. R. Feramisco. 1980. Microinjection and localization of a 130K protein in living fibroblasts: a relationship to actin and fibronectin. *Cell.* 19:587–595.

24. Feramisco, J. R., and S. H. Blose. 1980. Distribution of fluorescently labeled α-actinin in living and fixed fibroblasts. *J. Cell Biol.* 86:608–615.

25. Feramisco, J. R. 1979. Microinjection of fluorescently labeled α-actinin into living fibroblasts. *Proc. Natl. Acad. Sci. USA.* 76:3967–3971.

26. Kreis, T. E., and W. Birchmeier. 1980. Stress fiber sarcomeres of fibroblasts are contractile. *Cell.* 22:555–561.

27. Rungger, D., E. Rungger-Brändle, C. Chaponnier, and G. Gabbiani. 1979. Intranuclear injection of anti-actin antibodies into *Xenopus* oocytes blocks chromosome condensation. *Nature (Lond.).* 282:320–321.

28. Klymkowsky, M. W. 1981. Intermediate filaments in 3T3 cells collapse after intracellular injection of a monoclonal anti-intermediate filament antibody. *Nature (Lond.).* 291:249–251.

29. Lin, J. J.-C., and J. R. Feramisco. 1981. Disruption of the in vivo distribution of the intermediate filaments in fibroblasts through the microinjection of a specific monoclonal antibody. *Cell.* 24:185–193.

30. Mabuchi, I., and M. Okuno. 1977. The effect of myosin antibody on the division of starfish blastomeres. *J. Cell Biol.* 74:251–263.

31. Kiehart, D. P., I. Mabuchi, and S. Inoué. 1982. Evidence that myosin does not contribute to force production in chromsome movement. *J. Cell Biol.* 94:165–178.

32. Taylor, D. L., J. R. Blinks, and G. Reynolds. 1980. Contractile basis of ameboid movement. VIII. Aequorin luminescence during ameboid movement, endocytosis, and capping. *J. Cell Biol.* 86:599–607.

33. Wehland, J., M. Osborn, and K. Weber. 1980. Phalloidin associates with microfilaments after microinjection into tissue culture cells. *Eur. J. Cell Biol.* 21:188–194.

34. Wehland, J., and K. Weber. 1981. Actin rearrangement in living cells revealed by microinjection of a fluorescent phalloidin derivative. *Eur. J. Cell Biol.* 24:176–183.

35. Stockem, W., K. Weber, and J. Wehland. 1978. The influence of microinjected phalloidin on locomotion, protoplasmic streaming and cytoplasmic organization in Amoeba proteus and Physarum polycephalum. *Cytobiologie.* 18:114–131.

36. Götz von Olenhusen, K., and K. E. Wohlfarth-Bottermann. 1979. Evidence for actin transformation during the contraction-relaxation cycle of cytoplasmic actomyosin: cycle blockade by phalloidin injection. *Cell Tissue Res.* 196:455–470.

37. Wehland, J., M. Osborn, and K. Weber. 1977. Phalloidin-induced actin polymerization in the cytoplasm of cultured cells interferes with cell locomotion and growth. *Proc. Natl. Acad. Sci. USA.* 74:5613–5617.

38. Kiehart, D. P. 1981. Studies on the in vivo sensitivity of spindle microtubules to calcium ions and evidence for a vesicular calcium-sequestering system. *J. Cell Biol.* 88:604–617.

39. Gawlitta, W., W. Stockem, J. Wehland, and K. Weber. 1980. Pinocytosis and locomotion of amoebae. XV. Visualization of Ca^{++}-dynamics by chlorotetracycline (CTC) fluorescence during induced pinocytosis in living *Amoeba proteus. Cell Tissue Res.* 213:9–20.

40. Meeusen, R. L., J. Bennett, and W. Z. Cande. 1980. Effect of microinjected *N*-ethylmaleimide-modified heavy meromyosin on cell division in amphibian eggs. *J. Cell Biol.* 86:858–865.

41. Spudich, J. A., and S. Watt. 1971. The regulation of rabbit skeletal muscle contraction. *J. Biol. Chem.* 246:4866–4871.

42. Wang, Y.-L, and D. L. Taylor. 1980. Preparation and characterization of a new molecular cytochemical probe: 5-iodoacetamidofluorescein-labeled actin. *J. Histochem. Cytochem.* 28:1198–1206.

43. Bradford, M. M. 1976. A rapid and sensitive method for the quantitation of microgram quantities of protein utilizing the principle of protein-dye binding. *Anal. Biochem.* 72:248–254.

44. Taylor, D. L., J. Reidler, J. A. Spudich, and L. Stryer. 1981. Detection of actin assembly by fluorescence energy transfer. *J. Cell Biol.* 89:362–367.

45. Diacumakos, E. G. 1973. Methods for micromanipulation of human somatic cells in culture. *Methods Cell Biol.* 7:287–311.

46. Geiger, B. 1979. A 130K protein from chicken gizzard: its localization at the termini of microfilament bundles in cultured chicken cells. *Cell.* 18:193–205.

47. Pollard, T. D. 1981. Cytoplasmic contractile proteins. *J. Cell Biol.* 91(3, Pt. 2):156s–165s.

48. Geiger, B. 1981. The association of rhodamine-labelled α-actinin with actin bundles in demembranated cells. *Cell Biol. Int. Rep.* 5:627–634.

49. Gordon, W. E., III, and A. Bushnell. 1979. Immunofluorescent and ultrastructural studies of polygonal microfilament networks in respreading non-muscle cells. *Exp. Cell Res.* 120:335–348.

50. Abercrombie, M., and G. A. Dunn. 1975. Adhesions of fibroblasts to substratum during contact inhibition observed by interference reflection microscopy. *Exp. Cell Res.* 92:57–62.

51. Rubinstein, N., J. Chi, and H. Holtzer. 1976. Coordinated synthesis and degradation of actin and myosin in variety of myogenic and nonmyogenic cells. *Exp. Cell Res.* 97:387–393.